

Article

Effect of Accumulated Dust Conductivity on Leakage Current of Photovoltaic Modules

Yu Gao ^{1,2,*}, Fei Guo ¹, Haibo Tian ², Mengyuan Xue ¹, Yaoyang Jin ¹ and Baomiao Wang ¹

¹ School of Electrical and Control Engineering, Xi'an University of Science and Technology, Xi'an 710699, China; 13679199372@163.com (F.G.); xxldxld@163.com (M.X.); 15389391531@163.com (Y.J.); 15710429853@163.com (B.W.)

² School of Mechanical Engineering, Xi'an University of Science and Technology, Xi'an 710054, China; ttttian_74@163.com

* Correspondence: xkdgy@163.com

Abstract: Photovoltaic (PV) modules are often situated in hot and windy environments, such as deserts, where dust accumulation poses a significant problem. The build-up of dust can result in an increase in PV module leakage current, making the modules more vulnerable to potential-induced degradation (PID), ultimately leading to a reduction in the efficiency of PV power generation. In this study, we investigate the impact of dust accumulation on the surface of PV modules on leakage current. A dust model is developed based on the Arrhenius relation, taking into account the impact of temperature and density on dust conductivity. The equation for leakage current due to dust accumulation is derived based on the clean module leakage current equation. We undertake a simulation of natural conditions in a laboratory setting to analyze the impact of dust on the leakage current of photovoltaic modules. The results show the following: At high temperatures, the leakage current will significantly increase due to the elevated conductivity of the dust. The conductivity increased by 27.1%, 48.9%, 64.3%, and 118% for the four groups of dusty PV modules, respectively. Leakage current prediction has a better accuracy when dust is equated to series conductance. Dust can reduce the activation energy of PV modules by up to 3.48%.

Keywords: photovoltaic modules; dust accumulation; temperature; potential induce degradation



Citation: Gao, Y.; Guo, F.; Tian, H.; Xue, M.; Jin, Y.; Wang, B. Effect of Accumulated Dust Conductivity on Leakage Current of Photovoltaic Modules. *Energies* **2024**, *17*, 3116. <https://doi.org/10.3390/en17133116>

Academic Editor: Anastassios M. Stamatelos

Received: 23 May 2024

Revised: 17 June 2024

Accepted: 21 June 2024

Published: 25 June 2024



Copyright: © 2024 by the authors. Licensee MDPI, Basel, Switzerland. This article is an open access article distributed under the terms and conditions of the Creative Commons Attribution (CC BY) license (<https://creativecommons.org/licenses/by/4.0/>).

1. Introduction

China has vast desert areas, especially in the Northwest, where the annual solar irradiation exceeds 1700 kWh/m², making it an ideal location for constructing photovoltaic (PV) power plants [1]. However, in desertified areas, dust particles are a significant component of the air. This leads to an increase in dust deposition on the surface of PV modules, which significantly impacts the operation of desert PV plants. Dust can impact the power generation of PV modules through various factors, such as light transmission, temperature, and corrosion. When dust accumulates on the surface of PV panels, it significantly impacts PV power generation [2–5]. Burton P. D manually applied soil to photovoltaic panels and quantified the impact of the film on incident light transmission. The study's results revealed that various dust compositions result in diverse levels of degradation in PV cell performance [6]. Chanchang Y. N studied the impact of the accumulation of 13 different dust samples on PV performance. The results indicated that charcoal had the most significant degrading effect on PV performance, reducing the short-circuit current by approximately 98%, while salt appeared to have the least effect, at about 7% [7]. Alnasser T. M conducted a study on the impact of the accumulation of construction materials (such as sand, common cement, industrial gypsum, etc.) on the power output of photovoltaic modules. The findings of the study indicated that even small quantities of these materials accumulated on the PV module can reduce transmittance and decrease the power produced [8]. The movement of dust particles through the air, inter-particle collisions, and friction can lead to the charging

of particles [9]. Before the dust particles become completely static and accumulate on the photovoltaic panels, collision and friction processes between the particles and the panels are inevitably involved. Studies have demonstrated that the dynamic contact process between particles of varying sizes or compositions involves the exchange and transfer of charged microscopic particles, leading to the electrical charging of the particles [10]. Therefore, it is crucial to consider the impact of the conductive properties of the dust that accumulates on the surface of PV panels on PV modules. Temperature is one of the main factors affecting conductivity. Guo conducted a study on the influence of temperature on the electrical conductivity of graphite and quartz. The results demonstrated that an increase in temperature significantly enhances the electrical conductivity of both graphite and quartz [11]. Lu's study indicated that temperature is a critical factor influencing the conductivity of red clay. This is primarily demonstrated by the heightened activity of ions in the pore water resulting from an increased temperature, leading to an increase in the conductivity of red clay [12]. Han utilized the two-phase electrode method on sandy soil for an experimental determination of conductivity variation with temperature. The results indicated that the conductivity of the sandy soil increased with rising temperature, and the relationship between conductivity and temperature change exhibited a strong logarithmic correlation [13]. Mgaidi A modeled sand grains using the Arrhenius equation, taking into account parameters such as temperature, particle size, and the molar concentration of hydroxide ions. The experimental results conducted at various temperatures showed excellent agreement with the calculated data, with absolute root mean square (rms) deviations of less than 7% [14].

Potential-induced degradation (PID) is a significant factor that can lead to power degradation in PV modules. Research by Badran G revealed that PV modules may experience PID after 4–8 months of operation in various fields, resulting in a 27–39% reduction in power [15]. PID occurs when the high voltage interacts with environmental factors such as temperature and humidity, leading to power degradation in PV modules. The high voltage between the frame and the PV cell can cause sodium ions to leak from inside the PV module to other components, creating a leakage current that results in localized p-n junction failure of the PV cell [16]. Thus, the leakage current serves as a crucial indicator of PID [17]. A thorough understanding of the PID phenomenon and its improvement can be achieved by investigating the impact of different environmental conditions on the leakage current of photovoltaic modules. Various environmental elements like temperature, humidity (both inside and outside the module) [18], light levels [19], voltage, and system grounding affect the PV module leakage current. Building on Peck's model and extensive experimental data, Hacke P and colleagues developed a potential-induced degradation model for PV modules based on temperature and humidity [18]. Shiradkar simulated and analyzed the electric field distribution and leakage current distribution of PV modules under high voltage using finite element analysis [20]. Pan and team discovered that exposing the standard module to PID stress results in a higher composite current compared to the standard module, by analyzing the performance characteristics of PV modules with a dual diode equivalent model [21]. Moreover, Oh. W estimated the power loss rate induced by PID in the Busan and Miami regions based on temperature, humidity, and solar irradiation, revealing annual loss rates of 6.93% and 11.23%, respectively [22]. Bora B researched the impact of temperature, humidity, and voltage on PV module leakage current [23]. Islam M. A investigated the impact of dust accumulation on the leakage current of PV modules on the surface of PV modules in the laboratory. The results demonstrated an increase in leakage current values of 31.25%, 17.50%, and 32.35% for three groups of dust-accumulated PV modules [24]. This is because dust, salt, dew, and other factors can modify the conductive properties of the glass on the surface of a PV module [25]. Yilbas B discovered that dust particles are composed of unevenly distributed alkali and alkaline earth metals, oxygen, silicon, sulfur, and iron. Small dust particles ($\leq 0.5 \mu\text{m}$), due to their electrostatic charge, adhere to the surface of larger dust particles ($10 \leq 20 \mu\text{m}$) and accumulate on the PV glass surface. The presence of dust has a substantial impact on the chemical properties of the glass surface [26]. Suzuki

discovered that the leakage current of PV modules increases after the PV module surface has been exposed to salt spray treatment [27]. Ebneali F found that all test modules exhibited a susceptibility to leakage current at any temperature when conductive carbon (carbon layer) was applied to enhance the conductivity of the glass surface [28]. Sai R. studied the impact of altering the glass surface conductivity on the leakage current of photovoltaic modules by changing the type of conductive carbon applied to the glass surface. The research revealed that when the continuity of the glass surface conductivity is interrupted at the inner boundary of the frame, the module may not be affected by leakage current [29]. Khuram S proposed a method to reduce PID-induced power degradation by modifying the surface conductivity of PV modules. The interruption of the glass surface conductivity was accomplished by applying a hydrophobic material near the inner edge of the frame. The findings indicated that the module without any hydrophobic material experienced a 29% power loss after the PID stress test, while the module with the hydrophobic material only suffered a 15% power loss after the PID stress test [30].

Therefore, PV modules in desert and coastal areas often show higher leakage currents, attributed to the accumulation of dust that elevates the conductivity of the PV module surface [31–33]. Nagel N et al. conducted a study where they analyzed the distribution of localized leakage current density in a large-area PV module and measured the conductivity of the glass and EVA layers at different temperatures. Their results revealed that an increase in conductivity led to a significant shift in the local leakage current density by nearly 12 orders of magnitude at high temperatures of 85 °C and high humidity levels of 85%. However, the study did not consider the impact of dust accumulation on the PV module surfaces [34]. In another study, Peter Hacke investigated how the surface sheet resistance changed with humidity when different types of dust, such as sea salt, soot, and soil, were present. He found that the presence of sea salt deposits on the PV module surface led to a two- to tenfold increase in leakage current compared to when they were absent. Notably, the study did not account for the influence of temperature on the physical properties of dust, nor did it offer a relevant mathematical model [25]. Furthermore, Wang et al. developed a mathematical model to estimate dust density and conductivity [35]. However, the model did not consider the variability of dust conductivity under different environmental conditions, since it was developed based on constant humidity and temperature settings.

In summary, PID is a primary factor contributing to power degradation in PV modules and warrants careful attention. The leakage current increases as dust accumulates on the surface of the PV module, leading to a reduction in PV power output. Therefore, conducting a comprehensive study on the impact of dust on the leakage current of photovoltaic modules is crucial. This paper focuses on the high-temperature environment in desert regions as its background, modeling the natural accumulation of dust in the laboratory, and modeling the conductivity of dust by considering the impact of temperature and density on conductivity, to derive an equation for leakage current in photovoltaic modules after dust accumulation. This study aims to analyze the impact of dust on the leakage current of PV modules. This study provides a theoretical basis for the maintenance and replacement of PV modules in desert environments. By utilizing the dust leakage current model to determine cleaning and replacement schedules, significant improvements can be made to the lifetime and power output of PV modules.

2. Experiments and Methods

2.1. Leakage Current Modeling of Dust Accumulation Modules

In this section, the conductivity of dust is modeled using the Arrhenius relationship, taking into account both temperature and the quantity of dust. The leakage current equation for pristine PV modules is modified to provide the leakage current equation for PV modules with a dust accumulation.

2.1.1. Dust Modeling

The dust layer is created by the build-up of numerous dust particles. The conductivity of a dust layer differs from that of individual particles in that the conductive mechanism of particles includes surface conductivity and bulk conductivity, while the conductivity of a dust layer can be seen as a composite conductor created by numerous dust particles connected in series and parallel. As shown in Figure 1, the conductive process of the dust layer is the migration of carriers (usually ions) along the surfaces and interiors of numerous particles driven by the force of an electric field. Surface conductance refers to the conductance generated by ionic conduction through the liquid film on the surface of the particle, while bulk conductance is the conductance produced by ionic conduction within the particle [36].

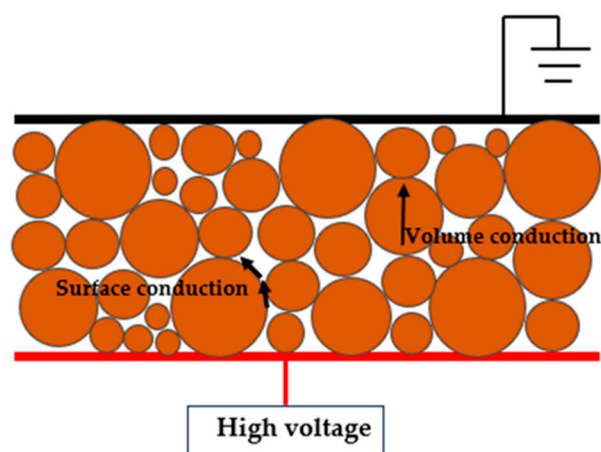


Figure 1. Volume and surface conductivity of dust layer.

From the analysis of the conductive mechanism of dust, it is apparent that as the temperature rises from a low level, water within the dust particles evaporates gradually from the interior towards the surface, resulting in the formation of a surface liquid film on the particle surfaces. Under these circumstances, current conduction in the dust layer primarily depends on the surfaces of the particles. As the temperature continues to rise, the water on the surface of the particles is gradually evaporated. With the decrease in water content through evaporation, the liquid film gradually disappears. At this time, the conduction of current in the dust layer is mainly dominated by ion migration within the particles. Elevated temperatures increase the electrical conductivity of electrons and ions within dust particles.

At the microscopic level, the relationship between conductivity and temperature for dust particles can be explained by the Nernst–Einstein equation. The Nernst–Einstein equation provides a quantitative description of electrical conductivity in the presence of charged particles [37], as depicted in Equation (1).

$$G = \frac{D \cdot c \cdot q^2}{k \cdot T} \quad (1)$$

where G is the conductivity of the charged particles; D is the diffusion coefficient of the charged particles; c is the charged particle content; q is the charge of the charged particles; k is the Boltzmann constant; and T is the temperature.

At the macroscopic level, the relationship between the conductivity and temperature of dust particles can be characterized using the Arrhenius equation, where the parameters in the equation are determined experimentally. The Arrhenius equation is frequently utilized to describe the temperature dependence of conductivity in electrolyte solution systems [38], as shown in Equation (2). According to Equation (2), it is evident that there is a positive

exponential relationship between dust conductivity and temperature, indicating that dust conductivity increases as temperature rises.

$$G = G_0 \cdot e^{-\frac{E}{kT}} \tag{2}$$

where G_0 is an empirical constant; E is the fitting parameter; k is Boltzmann’s constant; and T is the temperature (K).

Another factor influencing dust conductivity is its density, referring to the amount of dust accumulated on the PV module. The conductivity of dust on photovoltaic panels is complexified by the accumulation of large amounts of dust on their surfaces. Therefore, in this paper, dust is considered as a uniform thin layer with a specific volume that covers the surface of the PV module, as illustrated in Figure 2.

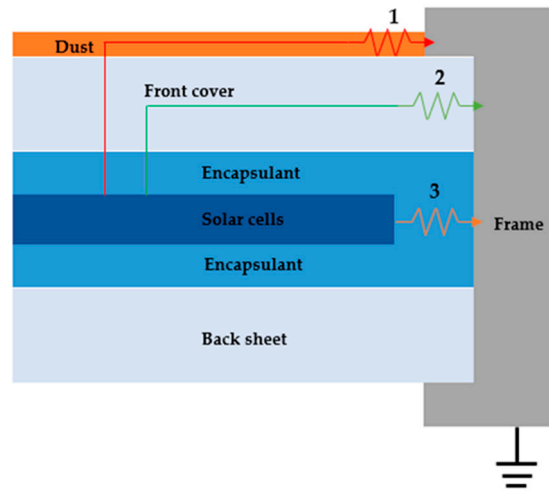


Figure 2. Conducting path of dusty PV module. Note: Path 1 represents the conductive path of the dust layer, while Path 2 signifies the conductive path of the glass on the surface of the photovoltaic module. Additionally, Path 3 denotes the conductive path of the PV module packaging material.

The volume of the dust layer is calculated indirectly based on the dust density and the surface area of the upper surface of the PV module. The specific calculation formula is as follows.

$$V_{eq} = S_{eq} \cdot \frac{m}{\rho \cdot S} \tag{3}$$

where V_{eq} is the equivalent conductive volume of the dust layer; S_{eq} is the equivalent conductive area of the dust; m is the mass of the dust; ρ is the mass density of the dust; S is the surface area of the PV module; and $m/(\rho \cdot S)$ is the thickness of the dust layer.

By combining Equations (2) and (3), we can derive an equivalent model for the dust layer, as shown in Equation (4).

$$G_d = S_{eq} \cdot \frac{m}{\rho \cdot S} \cdot e^{-\frac{E}{kT}} \tag{4}$$

where G_d is the conductivity of the dust.

2.1.2. Leakage Current Modeling of Dust Modules

Several studies have demonstrated that temperature and humidity influence the leakage current of clean photovoltaic modules, in accordance with the Arrhenius relationship [18,24]. Building on this, the Peck equation for leakage current can be derived, with temperature and humidity as variables, as illustrated in Equation (5).

$$i_0 = A \cdot e^{-\frac{E_a}{kT}} \cdot e^{B \cdot RH} \tag{5}$$

where i_0 is the magnitude of the leakage current of the junction net panel at -1000 V; A and B are empirical parameters; E_a is the activation energy parameter of the PV model; k is Boltzmann's constant; and T is the ambient temperature (K).

The relationship between leakage current and temperature can be established by defining the conductivity of the material in the PV modules as a function of temperature [39]. The temperature-dependent behavior of a material's conductivity is typically expressed through a mathematical model, as shown in Equation (6).

$$G = G_0 \cdot f(T) \quad (6)$$

where G is the conductivity of the material; G_0 is the model parameter; and T is the ambient temperature (K).

This study focuses solely on the surface glass and EVA layers of the PV module, as the leakage current through the back sheet layer is significantly lower compared to other layers [40]. As indicated in the literature [18], the conductivity of the PV module's glass and EVA layers for temperature complies with Equation (7).

$$G = G_0 \cdot e^{-\frac{E_a}{kT}} \quad (7)$$

where the G_0 of the PV glass and EVA is 25.2 S/cm and 0.6 S/cm, respectively; E_a is the activation energy of the material, and the E_a of the PV glass and EVA is 0.814 eV and 0.782 eV, respectively.

Based on the conductive path shown in Figure 2, the leakage current of a clean photovoltaic (PV) module passes through the surface glass and encapsulation material and then proceeds to the metal frame, ultimately flowing into the ground. Therefore, the total conductance (G_0) of the conductive channel in a clean PV module comprises the encapsulant conductance (G_v) and the surface glass conductance (G_s). For dust accumulation, it is also necessary to consider the conductivity of dust on PV modules. It is assumed that the dust conductance is in series with the total conductance of the clean PV module. Therefore, the total conductance (G_p) of the PV module after dust accumulation is calculated using Equation (8).

$$G_p = \frac{G_d \cdot (G_e + G_g)}{G_e + G_g + G_d} \quad (8)$$

where G_p is the total conductance of the dust accumulation assembly; G_d is the conductance of the dust; G_g is the conductance of the glass; and G_e is the conductance of the EVA.

The following relationship can be deduced from Ohm's law:

$$\frac{I_p}{I_0} = \frac{V \cdot G_p}{V \cdot G_0} \approx \alpha \left(\frac{G_d}{G_e + G_g + G_d} \right) \quad (9)$$

where I_0 is the leakage current of the clean PV module; I_p is the leakage current of dusty PV modules; V is a voltage of -1000 V applied to the PV cells; and α is the calculated adjustment factor, which is used to adjust the error between the relationships of G_d , G_g , and the G_e multiplier.

In conclusion, the leakage current of photovoltaic modules with accumulated dust can be determined using Equation (10).

$$I_p = A \cdot e^{-\frac{E_a}{kT}} \cdot e^{B \cdot RH} \cdot \alpha \left(\frac{G_d}{G_e + G_g + G_d} \right) \quad (10)$$

2.2. Experimental Section

The desert region's natural environment is characterized by windy sand and high temperatures. To study the conductivity of dust at different temperatures and densities, as well as the leakage currents of PV modules with accumulated dust under varying conditions, simulation experiments were conducted using a temperature-controlled test

chamber. The parameters in Equations (4) and (10) are determined by fitting the data collected from these experiments.

2.2.1. Experimental Equipment

The experimental setup involved monocrystalline silicon PV modules with a rated power of 20 W, conveniently sized at 420 mm × 350 mm × 17 mm to fit inside the experimental box for simulation studies. A YMY-H-type intelligent conductivity tester was employed to measure the dust's conductivity on the module's surface, while a S02-LB-ZF30 microammeter with an accuracy of 0.1 μA was used to measure the leakage current. Please refer to Table 1 for further details.

Table 1. Parameters of photovoltaic modules.

| Parameter | Value |
|---------------------------|----------------|
| Maximum working power/W | 20 |
| Maximum working current/A | 1.11 |
| Maximum working voltage/V | 18 |
| Short-circuit current/A | 1.28 |
| Open-circuit voltage/V | 21.61 |
| Dimension (L × W × T)/mm | 420 × 350 × 17 |

2.2.2. Dust Sources

The dust utilized in the experiments was collected from the natural accumulation on the surface of PV modules at a solar power station in Yulin City, Shaanxi Province. This dust, taken from the vicinity of the PV modules at the power station, was used as a simulated pollutant to replicate conditions closer to the natural operating environment of the modules. To prevent the particle size of the dust particles from affecting the experimental results, before conducting the experiment, the dust particles should be screened. The dust used in the experiment was sieved with 100-mesh and 150-mesh sieves, as illustrated in Figure 3, screening dust particles with a particle size < 100 μm for simulating ash coverings.



Figure 3. Illustration of 100-mesh and 150-mesh screens.

2.2.3. Experimental Methods

Sand dust collected from solar power plants was sieved to enhance particle uniformity for investigating the impact of dust accumulation on the leakage current of PV modules. Subsequently, dust particles with mass densities of 4.62, 9.90, 15.52, and 29.86 g/m² were

evenly distributed on the surfaces of PV modules from the same batch to simulate varying levels of dust accumulation. A control group consisted of an identical set of clean modules.

To simulate the high-voltage grounding state of PV modules during operation, a high voltage was introduced between the battery and the frame. The frame was linked to the positive pole of the power supply, while the positive and negative terminals of the module output were short-circuited and connected to the negative pole of the power supply. Concurrently, the magnitude of the leakage current was recorded. This experiment consists of two main components: the leakage current test and the dust conductivity test.

1. Leakage Current Test:

a. Both clean PV modules and dust-laden modules with dust accumulation levels of 4.62, 9.90, 15.52, and 29.86 g/m² were repeatedly placed in the test chamber. The chamber was maintained in a dark environment to prevent any influence from photocurrent on the results.

b. A ZGF-II-60 Kv/5 mA DC high-voltage generator was utilized to supply the necessary high voltage. The PV module frame was connected to the positive pole of the power supply, and after short-circuiting, the positive and negative terminals of the module outputs were connected to the negative pole of the power supply to simulate high-voltage stress on the PV module.

c. The temperature in the temperature-controlled test chamber could be adjusted within the range of 25 to 75 °C with increments of 5 °C. The humidity level was set at 20%. After setting the experimental temperature and ensuring the stability of the test chamber, the leakage current of the photovoltaic module was measured. Measure the leakage current three times at each temperature and calculate the average value to obtain the final result. This process was repeated for a total of five sets of trials, as shown in Figure 4.

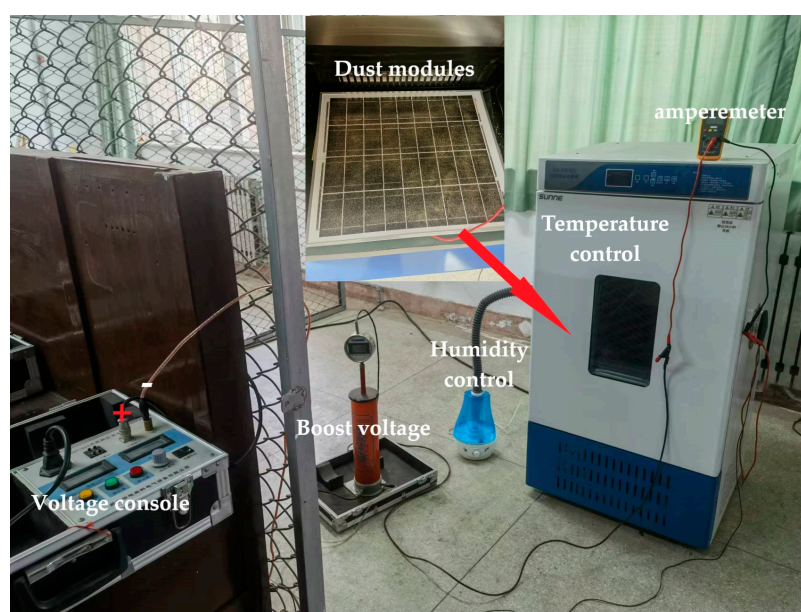


Figure 4. Leakage current measurement platform for dust accumulation components.

2. Dust conductivity test:

The conductivity test utilizes an YMY-H-type intelligent conductivity tester, which is designed in accordance with the standard [41]. This specialized meter is used to measure the conductivity of pollutants on the surface of power equipment with a precision of 0.1 μS/cm. The meter employs the two-electrode method for measuring conductivity. By applying a specific voltage between the two electrodes and measuring the resulting current, in conjunction with determining the distance between the electrodes and the area of the

electrode sheet, the conductivity of the pollutant solution can be accurately calculated through an internal chip control.

The weight of the dust collection cup was measured five times prior to the experiment using a high-precision electronic scale, LICHEN-FA2204, with an accuracy of 0.0001 g. The average value was then taken as the weight of the dust collection cup. The weight of the cup was 160.2993 g. The average conductivity of the solvents used (300 mL) was $2.1 \mu\text{S}/\text{cm}$ at a temperature range of 25 to 45 °C. This indicates that the chosen solvents are pure and will not interfere with the measurement of dust conductivity. The measuring equipment is shown in Figure 5. The conductivity test procedure is as follows.

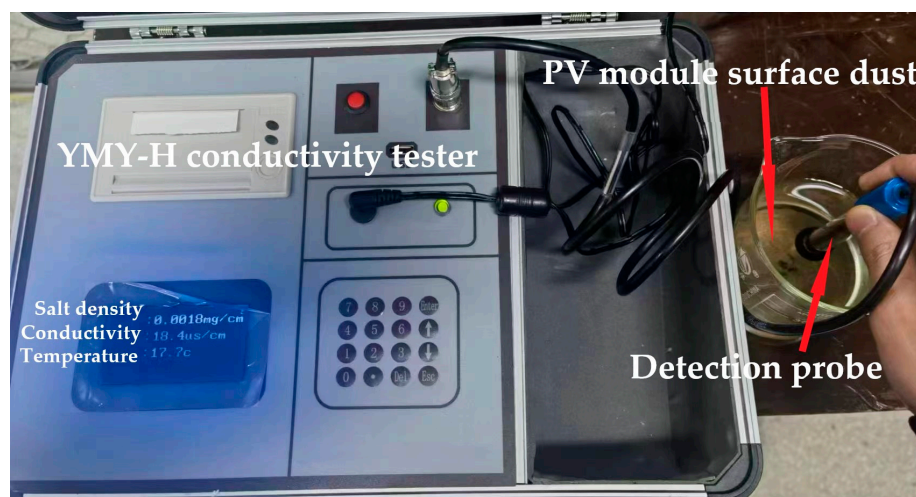


Figure 5. Dust conductivity measurement.

- a. After each set of leakage current tests, place the dust collection cup beneath the lower edge of the PV module. Utilize a small, clean brush to carefully sweep the dust into the dust collection cup within two to three passes.
- b. The dust collected is placed in an experimental chamber and dried at 70 °C for one hour to eliminate moisture from the dust.
- c. Use a high-precision electronic scale to measure the dust in the dust collection cup five times. Next, subtract the weight of the cup (160.2993 g) from each measurement and calculate the average of these five measurements to determine the mass of the dust in the cup.
- d. Add 300 mL of deionized water solvent to the dried dust, thoroughly mix, and allow it to stand for 2 min.
- e. Put the dust solution into the test chamber and heat it to a temperature range of 25~45 °C, increasing in increments of 5 °C.
- f. After the temperature reaches the preset value, use the YMY-H-type intelligent conductivity tester to measure the conductivity of dust at different temperatures. Subtract the reference value of solvent conductivity ($2.1 \mu\text{S}/\text{cm}$). Take three measurements and calculate the average value as the result.

3. Results and Discussion

3.1. Effect of Temperature on Dust Conductivity

Figure 6 illustrates the change in dust conductivity across a temperature range of 20 to 45 °C for measured PV module dust densities of 4.62, 9.90, 15.52, and 25.882 g/m². It can be observed from the figure that at dust densities of 4.62 g/m² and 9.90 g/m², there is minimal variation in dust conductivity between 20 and 35 °C, with a noticeable increase occurring between 35 and 45 °C. Additionally, for dust densities of 15.52 g/m² and 29.86 g/m², the conductivity surpasses that of lower densities at the same temperature, and the upward trend in conductivity gradually evens out with rising temperatures. The results depicted in Figure 6 indicate that the conductivity of dust at different densities

increases with temperature, with the conductivity rising as dust density increases, although the impact of temperature remains more significant. Dust exhibits lower conductivity at lower temperatures, escalating as the temperature rises. When the temperature escalates from 20 °C to 45 °C, the difference between the minimum and maximum conductivity values for various dust densities spans two orders of magnitude.

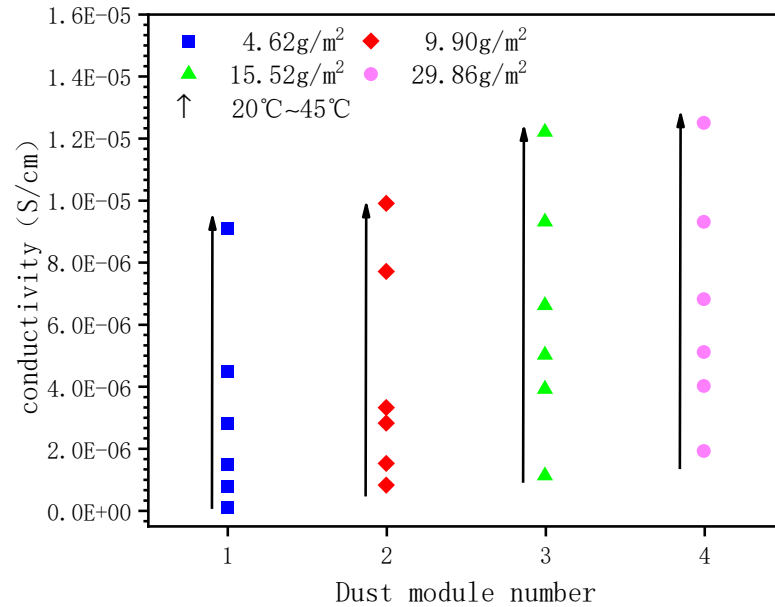


Figure 6. Variation in conductivity with temperature for different dust densities.

The results of experiments on dust conductivity indicate that temperature significantly influences dust conductivity. Hence, a quantitative investigation into the relationship between dust conductivity and temperature was undertaken. By applying the Arrhenius relationship, a mathematical model correlating dust conductivity with temperature was formulated. The approach involved taking the logarithm of the recorded conductivity data and establishing the relationship between $\ln(G_d)$ and $1/T$ in Equation (4). In Figure 7, the fitting results of the experimental data are presented, revealing that the logarithm of conductivity exhibits a linear correlation with the reciprocal of temperature, thereby satisfying the Arrhenius relationship. This demonstrates the viability of the model proposed in this study for describing the relationship between dust conductivity and temperature.

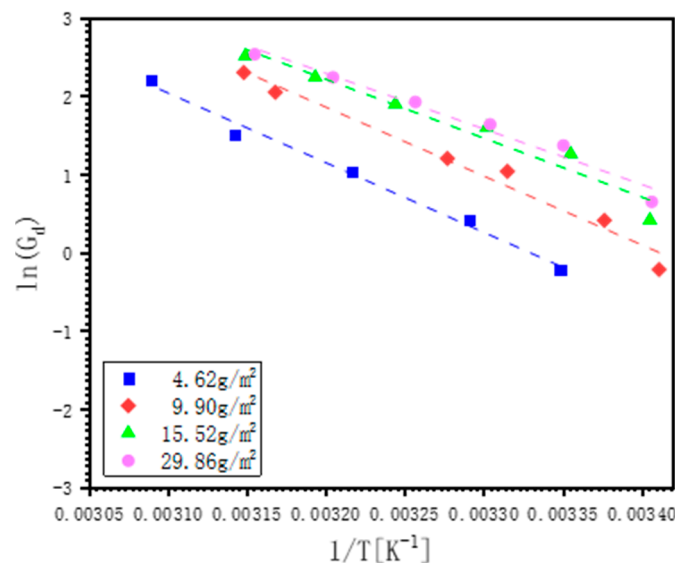


Figure 7. Fitting result of $\ln(G_d)$ and $1/T$.

The data from the four sets of dust conductivity versus temperature curves shown in Figure 7 were analyzed to fit the curves to Equation (4) and derive the parameters for the dust conductivity model. The R^2 values for the conductivity model fitting at four different dust densities (4.62 g/m^2 , 9.90 g/m^2 , 15.52 g/m^2 , and 29.86 g/m^2) were found to be 0.9889, 0.9772, 0.9498, and 0.9701, respectively.

3.2. Effect of Dust Accumulation on Module Leakage Current

The dust in the desert mainly consists of quartz, which has weak thermal conductivity, a small heat capacity, and a limited ability to equalize temperature differences between levels. When dust accumulates on the surface of a PV module, the heat absorbed by the sand and dust dissipates more slowly, leading to an increase in the thermal resistance of the PV module. This, in turn, reduces the heat dissipation performance of the module, causing its temperature to rise.

Experimental data shown in Figure 8 illustrate the leakage current measured for PV modules at various ash accumulation densities: 0 g/m^2 , 4.62 g/m^2 , 9.90 g/m^2 , 15.52 g/m^2 , and 29.86 g/m^2 , respectively. From the figure, it is observed that within the temperature range of 20 to $45 \text{ }^\circ\text{C}$, there is no significant change in the leakage current among modules with different dust densities. However, between 50 and $60 \text{ }^\circ\text{C}$, there is a slight increase in leakage current with rising dust levels and temperature compared to clean modules. As the temperature reaches 65 to $75 \text{ }^\circ\text{C}$, the leakage current of the dust-laden modules begins to substantially escalate, with the maximum increase being 27.1%, 48.9%, 64.3%, and 118.0% for the four groups of dust accumulation modules, respectively.

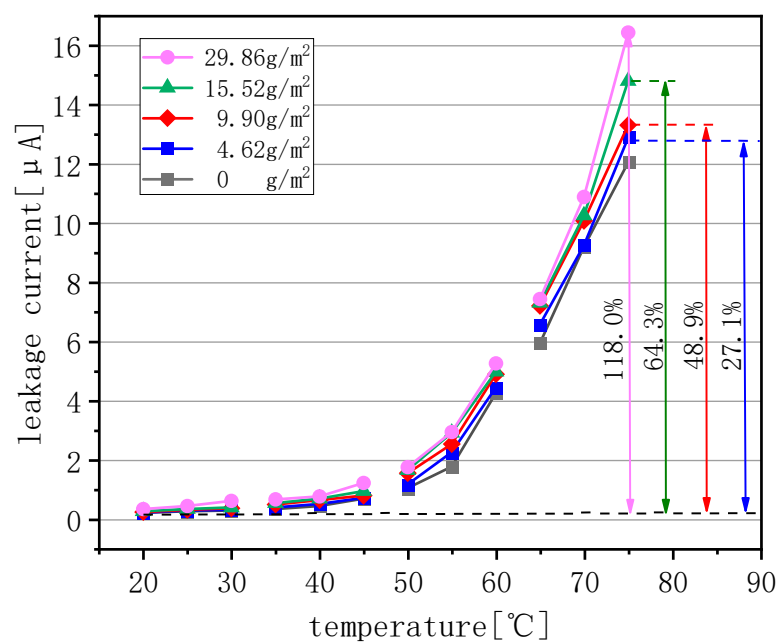


Figure 8. Leakage current of dust accumulation modules at different temperatures.

In desert regions, midday temperatures often exceed $50 \text{ }^\circ\text{C}$, reaching up to $70 \text{ }^\circ\text{C}$ in the summer [42], indicating that in such high-temperature desert environments, PV modules with dust accumulations will experience higher leakage currents compared to those in normal regions. Consequently, the elevated leakage current caused by dust accumulation in PV modules within desert areas could potentially lead to the potential-induced degradation of the modules.

Dust primarily influences the leakage current of PV modules through its conductivity. As discussed in the previous section, the conductivity of dust exhibits significant variations at different temperatures. Therefore, when modeling dust conductivity, it is essential to consider not only the linear relationship with density but also the influence of temperature.

To establish the leakage current equation for a dusty module, the model parameters of the leakage current equation for a clean module—denoted as A and B in Equation (5)—are required. Figure 9 illustrates the fitting results of the leakage current for a clean module, yielding the parameters A and B as 57.5659 and 1.2624, respectively. Additionally, the activation energy E_a is determined to be 0.8035.

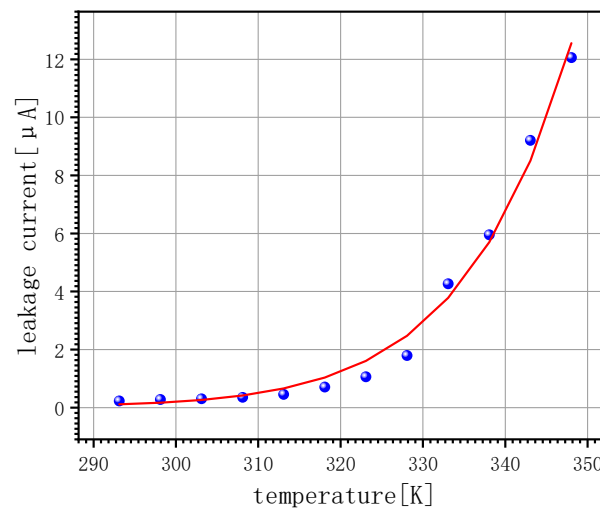


Figure 9. Leakage current fitting results for clean PV module.

Figure 10 provides a comparison of the fitting effects of utilizing the dust conductivity model proposed in this paper and a model that only takes into account the density of the leakage currents for four groups of measured dust accumulation assemblies. The analysis of Figure 10 indicates that the leakage current equation for dust accumulation components proposed in this paper, which considers both dust accumulation density and temperature, accurately predicts the leakage current. In contrast, the leakage current equation that only considers the dust accumulation density performs poorly in predicting the leakage current.

When the dust density on the surface of a PV module is 4.62 g/m^2 , the leakage current predicted by the density model performs well in the temperature range of $20\text{--}45 \text{ }^\circ\text{C}$. However, the predictive capability deteriorates as the temperature rises further. This decline is primarily attributed to the increase in dust conductivity at higher temperatures, causing the density model to lag in tracking the upward trend in leakage current. Additionally, the density model tends to underestimate the leakage current when there is less dust present. The results depicted in Figure 10b–d, with dust densities of 9.90 g/m^2 , 15.52 g/m^2 , and 29.86 g/m^2 , respectively, demonstrate that the density model can accurately predict the leakage current at lower temperatures where dust conductivity is influenced by temperature characteristics. However, as the temperature increases, the model's predictive accuracy significantly diminishes. Furthermore, an increase in dust density leads to the density model generally overestimating the leakage current compared to the actual values.

Comparing the three error evaluation metrics, namely, mean absolute percentage error (MAPE), mean absolute error (MAE), and root mean square error (RMSE), as calculated in Table 2, reveals that the error of the density model decreases somewhat with an increase in dust density. However, the density–temperature model exhibits a similar decrease in error as dust density increases. Furthermore, the average values of the errors are both above and below 0.2, indicating they are smaller than those of the density model. In conclusion, the leakage current equation for dust accumulation in PV modules proposed in this paper demonstrates better predictive capability for the leakage current in the presence of dust accumulation. This improvement can be attributed to the model's incorporation of both dust density and temperature effects on conductivity, leading to enhanced predictability.

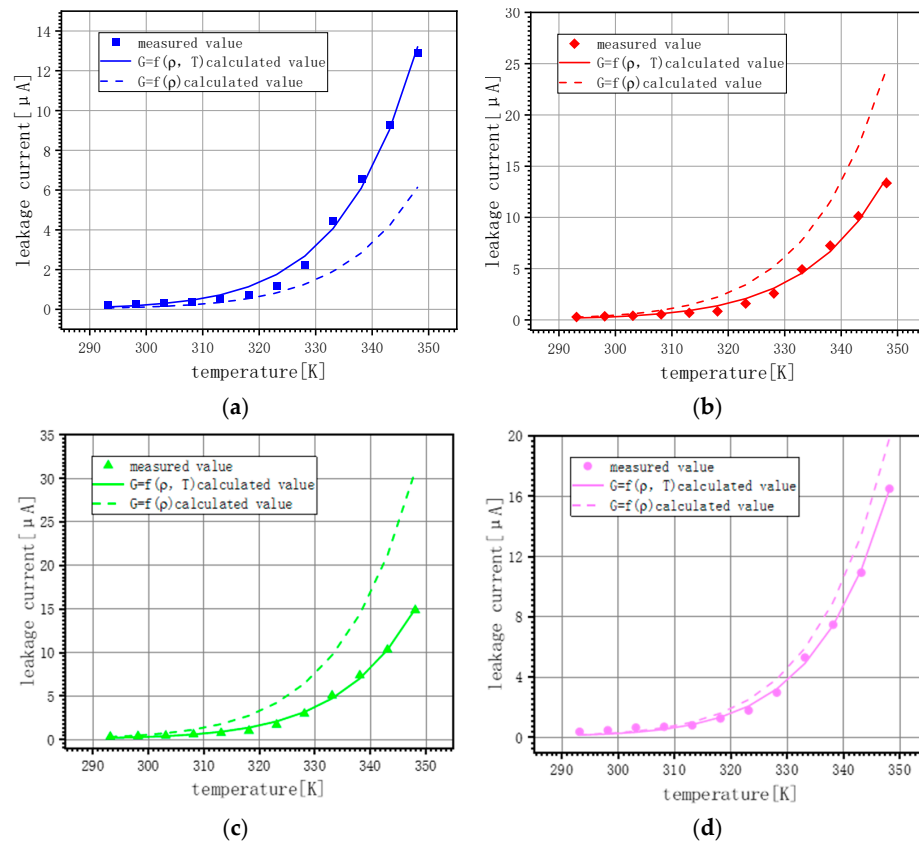


Figure 10. A comparison of the fitting effect of the temperature–density model and the density model on the leakage current of dust accumulation photovoltaic modules. The solid line is the temperature–density model. The dashed line is the density model. (a) The dust density is 4.62 g/cm²; (b) the dust density is 9.90 g/cm²; (c) the dust density is 15.52 g/cm²; (d) the dust density is 29.86 g/cm².

Table 2. Error indicators for different models.

| Dust Density (g/m ²) | Model | MAPE | MAE | RMSE |
|----------------------------------|-------|-----------|----------|----------|
| 4.62 | A | 0.255664 | 0.279962 | 0.328178 |
| | B | 0.515372 | 1.718467 | 2.791345 |
| | C | 0.533572 | 0.80608 | 1.047609 |
| 9.90 | A | 0.224359 | 0.32829 | 0.387076 |
| | B | 1.0133125 | 4.014174 | 6.243343 |
| | C | 0.572852 | 1.016038 | 1.29382 |
| 15.52 | A | 0.178263 | 0.185278 | 0.225931 |
| | B | 1.013313 | 4.014174 | 6.243343 |
| | C | 0.475199 | 0.751665 | 0.925778 |
| 29.86 | A | 0.207873 | 0.188929 | 0.218409 |
| | B | 0.303403 | 0.901657 | 1.341737 |
| | C | 0.44248 | 0.644423 | 0.744001 |

Note: A is the temperature–density model; B is the density model; and C is the parallel temperature–density model.

3.3. Connection Mode of Dust and Photovoltaic Module

The leakage current in PV modules primarily arises from the creation of a loop involving the encapsulation material (EVA), surface glass, and metal frame due to the presence of Na⁺ ions in the surface glass under reverse bias conditions, leading to the generation of leakage current [43]. While extensive research has focused on the internal leakage current pathways within PV modules, the influence of dust on these pathways remains unclear. This study assumes that the impact of accumulated dust is akin to introducing

a conductor in series with the module. Here, this section demonstrates that the effect of accumulated dust on leakage current can be likened to a series conductor by contrasting dust accumulation with a parallel conductor.

If the impact of dust on the leakage current pathway is analogous to parallel conductance, the total conductance of the PV module following dust accumulation can be represented by Equation (11).

$$G_P = G_e + G_g + G_d \quad (11)$$

Figure 11 presents the comparison of prediction results from experimental data using the dust module leakage current equations derived by treating dust as a parallel connection in Equation (8) and in a series connection in Equation (11), respectively. Upon scrutinizing the comparison outcomes, it is evident that the leakage current equation can reasonably forecast the leakage current value when the dust is equated to a parallel connection. However, the prediction error is marginally greater in comparison to the series connection equivalence. The mean absolute percentage error (MAPE), mean absolute error (MAE), and root mean square error (RMSE) of the two models across the four datasets are detailed in Table 2. Specifically, the mean values of MAPE and MAE for the series model stand at 0.234254 and 0.245615, respectively, whereas those for the parallel model are 0.506026 and 0.804552. These results indicate that the series model's predicted values align more closely with the actual leakage current. Additionally, the average RMSE value for the series model, at 0.289899, significantly outperforms the parallel model's RMSE of 1.0028, highlighting that the series model's predictions exhibit less deviation from the true value. Therefore, this analysis suggests that the role of dust in the leakage process of PV modules can be accurately represented as conductance in series.

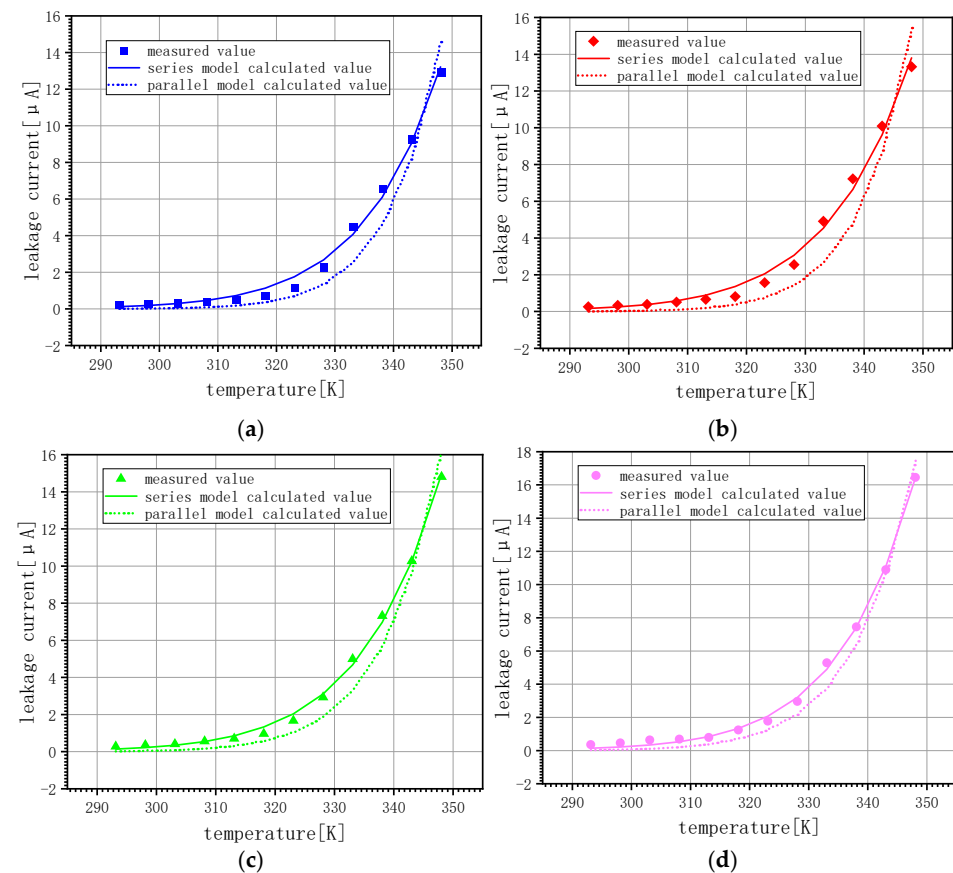


Figure 11. The dust equivalent is the comparison of the fitting effect of series conductance and parallel conductance to the leakage current of dust accumulation photovoltaic modules. The solid lines are in series. The dashed lines are in parallel. (a) The dust density is 4.62 g/cm²; (b) the dust density is 9.90 g/cm²; (c) the dust density is 15.52 g/cm²; (d) the dust density is 29.86 g/cm².

3.4. Effect of Dust on the Activation Energy of the Photovoltaic Module

The activation energy (E_a) serves as a crucial indicator of the likelihood of degradation occurring within a PV module. If the actual activation energy of a PV cell surpasses E_a , the module becomes vulnerable to physical and chemical reactions within the module, resulting in power degradation of the PV cell. Activation energy E_a is determined by the module's material, size, and external environment (including ambient humidity, surface condition, etc.) but remains relatively unaffected by ambient temperature. As demonstrated in Equation (5), due to the exponential function's inherent characteristics, even a slight alteration in the activation energy in the order of 0.01 eV can exert a substantial impact on the leakage current. The PV modules utilized in this study are sourced from the same production batch, thus eliminating the material composition of the module itself as a variable. The ambient humidity is held constant, with dust being the sole variable. The selection of activation energy values aims to scrutinize the impact of dust on the internal dynamics of the PV cell.

Figure 12 illustrates the relationship between the activation energy E_a of PV modules and dust density. The graph indicates that the activation energy E_a of dust-accumulating PV modules follows a pattern of initially decreasing and then increasing, although overall it remains lower than that of clean PV modules.

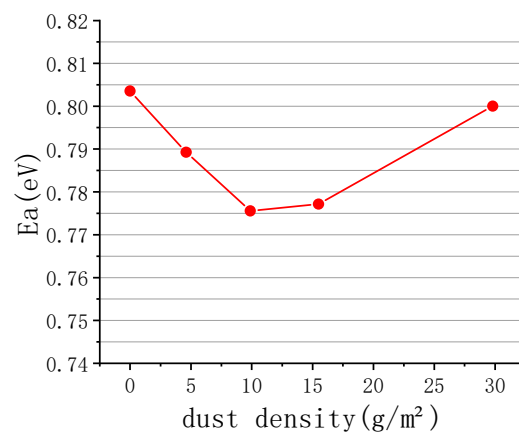


Figure 12. The activation energy E_a of photovoltaic modules varies with different dust densities.

When there is a small amount of dust accumulation on the PV module, it decreases the activation energy, potentially causing module leakage. In such cases, the limited amount of dust fails to establish a path for the leakage current, resulting in the current primarily flowing through the PV module's interior to the grounding frame. As the dust on the PV module's surface reaches a certain level, the activation energy of the module increases due to the conductivity of the accumulated dust being significantly higher (around 10^{-6}) compared to the internal materials and surface glass of the PV module (ranging from 10^{-12} to 10^{-10}). Consequently, the leakage current predominantly flows through the path formed by the dust. Therefore, dust accumulation reduces the activation energy of PV modules, making modules more prone to leakage and leading to decreased PV power output. The maximum reduction in the activation energy of a PV module due to dust accumulation is 3.48%.

4. Conclusions

In this study, the dust conductivity and leakage current of photovoltaic modules were experimentally measured. A dust conductivity model that takes into account temperature and density was developed. The equation for the leakage current of a photovoltaic module with accumulated dust was derived using the dust model. The study of this paper can lead to the following main conclusions:

1. The experimental findings have demonstrated a significant increase in dust conductivity at higher temperatures. Consequently, the accumulation of dust on the surface of PV

panels results in an elevated leakage current. Specifically, the maximum increase in leakage current is 27.1%, 48.9%, 64.3%, and 118% when the density of dust accumulation on the surface of PV modules is 4.62 g/m², 9.90 g/m², 15.52 g/m², and 29.86 g/m², respectively.

2. The variation of dust conductivity with temperature is in line with the Arrhenius relationship. The leakage current equation obtained using the established dust model accurately predicts the leakage current during dust accumulation on the surface of the PV module assembly. The maximum values for the three error analysis metrics (MAPE, MAE, RMSE) are 0.25567, 0.32829, and 0.32818, respectively.

3. Equating the connection relationship between dust and the PV module as a series interaction provides a higher accuracy in predicting leakage current compared to a parallel interaction.

4. Dust accumulation reduces the activation energy of PV modules, resulting in a lower energy requirement for leakage to occur and thus increasing the likelihood of leakage. The maximum decrease in activation energy due to dust is 3.48%.

5. For photovoltaic (PV) panels located in desert areas, it is important to minimize the increase in leakage current caused by dust. When the temperature exceeds 50 °C, it is crucial to promptly remove any accumulated dust.

Author Contributions: Writing—original draft preparation, Y.G. and F.G.; project administration, funding acquisition, H.T.; data curation, M.X. and Y.J.; investigation, B.W. All authors have read and agreed to the published version of the manuscript.

Funding: This research was funded by the National Natural Science Foundation of China (NSFC) and the General Project (Industrial Field) of Shaanxi Provincial Key Research and Development Program, grant numbers 52174149 and 2022GY-241.

Data Availability Statement: The data that support the findings of this study are available from the corresponding author, Y.G., upon reasonable request.

Conflicts of Interest: The authors declare no conflict of interest.

References

1. Zong, S.; Weicai, Z.; Zhiyong, C. Modeling analysis of cleaning strategy for photovoltaic power plants in Northwest China based on K-means algorithm and ash accumulation loss coefficient. *Sol. Energy* **2023**, *12*, 67–73.
2. Mingming, Z.; Dan, Z.; Bo, G.; Shuai, W.; Wu, L. Study on the effect of desert environment on photovoltaic modules. *J. Sol. Energy* **2020**, *41*, 365–370.
3. Wenshuai, Z.; Shuai, W.; Kai, W. Impact of ash accumulation on photovoltaic module power generation and planning of ash removal cycle. *South Agric. Mach.* **2022**, *53*, 122–126. [[CrossRef](#)]
4. Huifeng, N.; Rongzhan, C.; Weizhi, W. Experimental study on the effect of ash accumulation on photovoltaic power generation and dust removal effect. *J. Sol. Energy* **2020**, *41*, 120–125.
5. Shengjie, W.; Rui, T.; Ling, G. Research on the ash accumulation characteristics of photovoltaic module and its transmission attenuation. *J. Agric. Eng.* **2019**, *35*, 242–250. [[CrossRef](#)]
6. Burton, P.D.; King, B.H. Application and characterization of artificial grime for photovoltaic soiling studies. *IEEE J. Photovolt.* **2013**, *4*, 299–303. [[CrossRef](#)]
7. Chanchangi, Y.N.; Ghosh, A.; Sundaram, S.; Mallick, T.K. An analytical indoor experimental study on the effect of soiling on PV, focusing on dust properties and PV surface material. *Sol. Energy* **2020**, *203*, 46–68. [[CrossRef](#)]
8. Alnasser, T.M.; Mahdy, A.M.; Abass, K.I.; Chaichan, M.T.; Kazem, H.A. Impact of dust ingredient on photovoltaic performance: An experimental study. *Sol. Energy* **2020**, *195*, 651–659. [[CrossRef](#)]
9. Xie, L.; Li, J.; Liu, Y. Review on charging model of sand particles due to collisions. *Theor. Appl. Mech. Lett.* **2020**, *10*, 276–285. [[CrossRef](#)]
10. Wang, J. Studies on the Contact Electrification and Electrostatic Force Between Atmospheric Deosition and Photovoltaic Panels. Master's Thesis, Ningxia University, Ningxia, China, 2023; p. 0424. [[CrossRef](#)]
11. Yingxing, G.; Tao, Z.; Jun, Z. Numerical simulation of electrical conductivity on the graphite-quartz model and its geophysical application. *Geophys. J.* **2021**, *64*, 4031–4042. [[CrossRef](#)]
12. Jing, L. Preliminary Study on Resistivity Characteristics and Influencing Factors of Artificially Contaminated Soil. Master's Thesis, Inner Mongolia University of Science and Technology, Inner Mongolia, China, 2023. [[CrossRef](#)]
13. Lihua, H.; Songyu, L.; Yanjun, D. Experiment study on the effect of temperature on electrical resistivity of contaminated soils. *Geotech. Eng.* **2007**, *06*, 1151–1155. [[CrossRef](#)]

14. Mgaidi, A.; Jendoubi, F.; Oulahna, D.; El Maaoui, M.; Dodds, J.A. Kinetics of the dissolution of sand into alkaline solutions: Application of a modified shrinking core model. *Hydrometallurgy* **2004**, *71*, 435–446. [[CrossRef](#)]
15. Badran, G.; Dhimish, M. Field study on the severity of photovoltaic potential induced degradation. *Sci. Rep.* **2022**, *12*, 22094. [[CrossRef](#)] [[PubMed](#)]
16. Dhimish, M.; Badran, G. Field Study of Photovoltaic Systems with Anti-Potential-Induced-Degradation Mechanism: UVE, EL, and Performance Ratio Investigations. *Photonics* **2023**, *10*, 225. [[CrossRef](#)]
17. Voswinckel, S.; Mikolajick, T.; Wesselak, V. Influence of the active leakage current pathway on the potential induced degradation of CIGS thin film solar modules. *Sol. Energy* **2020**, *197*, 455–461. [[CrossRef](#)]
18. Hacke, P.; Spataru, S.; Terwilliger, K.; Perrin, G.; Glick, S.; Kurtz, S.; Wohlgemuth, J. Accelerated testing and modeling of potential induced degradation as a function of temperature and relative humidity. In Proceedings of the Photovoltaic Specialist Conference, IEEE, New Orleans, LA, USA, 14–19 June 2015; p. 0601. [[CrossRef](#)]
19. Hacke, P.; Terwilliger, K.; Glick, S.; Tamizhmani, G.; Tatapudi, S.; Stark, C.; Koch, S.; Weber, T.; Berghold, J.; Hoffmann, S.; et al. Interlaboratory study to determine repeatability of the damp-heat test method for potential-induced degradation and polarization in crystalline silicon photovoltaic modules. *IEEE J. Photovolt.* **2017**, *5*, 94–101. [[CrossRef](#)]
20. Shiradkar, N.; Schneller, E.; Dhere, N.G. Finite element analysis based model to study the electric field distribution and leakage current in PV modules under high voltage bias. *SPIE Sol. Energy Technol.* **2013**, *8825*, 88250G-2. [[CrossRef](#)]
21. Pan, Z.; Ju, X.; Cheng, X.; Chen, C.; Dong, Y. Modeling Recombination in PID-affected N-type Mono-crystalline Silicon Solar Module. In Proceedings of the 2018 IEEE 7th World Conference on Photovoltaic Energy Conversion, Waikoloa, HI, USA, 10–15 June 2018; pp. 0462–0466. [[CrossRef](#)]
22. Oh, W.; Bae, S.; Chan, S.I. Field degradation prediction of potential induced degradation of the crystalline silicon photovoltaic modules based on accelerated test and climatic data. *Microelectron. Reliab.* **2017**, *76*, 596–600. [[CrossRef](#)]
23. Bora, B.; Mondal, S.; Prasad, B. Accelerated stress testing of potential induced degradation susceptibility of PV modules under different climatic conditions. *Sol. Energy* **2021**, *223*, 158–167. [[CrossRef](#)]
24. Islam, M.A.; Hasanuzzaman, M.; Abd Rahim, N. Effect of different factors on the leakage current behavior of silicon photovoltaic modules at high voltage stress. *IEEE J. Photovolt.* **2018**, *8*, 1259–1265. [[CrossRef](#)]
25. Hacke, P.; Burton, P.; Hendrickson, A. Effects of photovoltaic module soiling on glass surface resistance and potential-induced degradation. In Proceedings of the 2015 IEEE 42nd Photovoltaic Specialist Conference (PVSC), New Orleans, LA, USA, 14–19 June 2015; pp. 1–4. [[CrossRef](#)]
26. Yilbas, B.S.; Ali, H.; Khaled, M.M.; Al-Aqeeli, N.; Abu-Dheir, N.; Varanasi, K.K. Influence of dust and mud on the optical, chemical and mechanical properties of a pv protective glass. *Sci. Rep.* **2015**, *5*, 15833. [[CrossRef](#)] [[PubMed](#)]
27. Suzuki, S.; Nishiyama, N.; Yoshino, S.; Ujiro, T.; Watanabe, S.; Doi, T.; Masuda, A.; Tanahashi, T. Acceleration of potential-induced degradation by salt-mist preconditioning in crystalline silicon photovoltaic modules. *Jpn. J. Appl. Phys.* **2015**, *54*, 08K08. [[CrossRef](#)]
28. Ebneali, F.; Sai, T.; GovindaSamy, T.M. Potential induced degradation of pre-stressed photovoltaic modules: Influence of polarity, surface conductivity and temperature. In Proceedings of the 2013 IEEE 39th Photovoltaic Specialists Conference (PVSC), Tampa, FL, USA, 16–21 June 2013; pp. 1548–1553. [[CrossRef](#)]
29. Vasista, S.R. Potential Induced Degradation (PID) of Pre-Stressed Photovoltaic Modules: Effect of Glass Surface Conductivity Disruption. Master's Thesis, Arizona State University, Tempe, AZ, USA, 2012. [[CrossRef](#)]
30. Shahzad, K.; Khalid, M.S.; Amin, A.; Israr, K.; Khan, R.; Oh, J.; Tatapudi, S.; TamizhMani, G. Addressing potential-induced degradation of field-installed PV modules by reducing surface conductivity. *New Concepts Sol. Therm. Radiat. Convers. Reliab.* **2018**, *10759*, 30–35. [[CrossRef](#)]
31. Zhang, J.; Cao, D.; Diahm, S. Research on potential induced degradation (PID) of polymeric backsheets in PV modules after salt-mist exposure. *Sol. Energy* **2019**, *188*, 475–482. [[CrossRef](#)]
32. Hoffmann, S.; Koehl, M. Effect of humidity and temperature on the potential-induced degradation. *Prog. Photovolt. Res. Appl.* **2014**, *22*, 173–179. [[CrossRef](#)]
33. Ping, W.; Wei, D.; Haining, Z.; Chunlai, L. Study on the influence of surface area ash on leakage current and decay life of photovoltaic modules. *J. Sol. Energy* **2019**, *40*, 119–125.
34. Nagel, H.; Glatthaar, M.; Glunz, S.W. Quantitative assessment of the local leakage current in PV modules for degradation prediction. In Proceedings of the 31st European Photovoltaic Solar Energy Conference and Exhibition, Hamburg, Germany, 14–18 September 2015; pp. 1825–1829. [[CrossRef](#)]
35. Ping, W.; Meiya, K.; Wei, D. The effect of pollutants on leakage current and power degradation of photovoltaic modules. *Renew. Energy* **2020**, *146*, 2668–2675. [[CrossRef](#)]
36. Hao, Z. Study on Particle Removal Enhancement in the Electrostatic Field by Dust Layer Adjustment. Master's Thesis, Zhejiang University, Hangzhou, China, 2021. [[CrossRef](#)]
37. Li, B.C.; Sun, S.H. Study on conductivity temperature relationship based on Nernst-Einstein and Arrhenius Equations. *J. Imm. Mong. Univ. Technol.* **2022**, *41*, 475–480. [[CrossRef](#)]
38. Leiqiang, Z. Volumetric, viscosity, Study on Volume, Viscosity Properties and Electrical Conductivity of Quaternary Ammonium Electrolyte Solution. Master's Thesis, Nanchang University, Nanchang, China, 2022.

39. Anagha, E.R.; Pratti, D.; Kulkarni, S.V. Modeling of Leakage Currents in c-Si PV Modules and Investigation of their Arrhenius Behavior. In Proceedings of the 2020 IEEE 47th Photovoltaic Specialists Conference (PVSC), Calgary, AB, Canada, 15 June–21 August 2020; pp. 1105–1109. [[CrossRef](#)]
40. Bauer, J.; Naumann, V.; Grosser, S. On the mechanism of potential-induced degradation in crystalline silicon solar cells. *Phys. Status Solidi-Rapid Res. Lett.* **2012**, *6*, 331–333. [[CrossRef](#)]
41. GB/T 26218.1-2010; Selection and Dimensioning of High-Voltage Insulators Intended for Use in Polluted Conditions—Part 1: Definitions, Information and General Principles. Standardization Administration of China: Beijing, China, 2011.
42. Hu, W.W. Research on Surface Thermal Characteristics and Temperature Field of Photovoltaic Modules in Desertified Areas. Master's Thesis, Ningxia University, Ningxia, China, 2023; p. 1214. [[CrossRef](#)]
43. Guosheng, W.; Qing, H.; Lili, J. Characteristics of summer surface temperature differences in the sandy ridges of the Taklamakan Desert. *Desert Oasis Meteorol.* **2022**, *16*, 13–14.

Disclaimer/Publisher's Note: The statements, opinions and data contained in all publications are solely those of the individual author(s) and contributor(s) and not of MDPI and/or the editor(s). MDPI and/or the editor(s) disclaim responsibility for any injury to people or property resulting from any ideas, methods, instructions or products referred to in the content.